Journal of Biomolecular NMR, **20:** 39–47, 2001.
KLUWER/ESCOM

Measurement and application of ^{1}H-^{19}F dipolar couplings in the structure determination of 2′-fluorolabeled RNA

Burkhard Luy & John P. Marino*
Center for Advanced Research in Biotechnology of the University of Maryland, Biotechnology Institute and the National Institute for Standards and Technology, 9600 Gudelsky Drive, Rockville, MD 20850, U.S.A.

Received 26 December 2000; Accepted 23 February 2001

Key words: dipolar couplings, dipolar-TOCSY, E.COSY, fluorine, MOCCA, RNA

Abstract

Residual dipolar couplings can provide powerful restraints for determination and refinement of the solution structure of macromolecules. The application of these couplings in nucleic acid structure elucidation can have an especially dramatic impact, since they provide long-range restraints, typically absent in NOE and *J*-coupling measurements. Here we describe sensitive X-filtered-E.COSY-type methods designed to measure both the sign and magnitude of long-range ^{1}H-^{19}F dipolar couplings in selectively fluorine labeled RNA oligonucleotides oriented in solution by a liquid crystalline medium. The techniques for measuring ^{1}H-^{19}F dipolar couplings are demonstrated on a 21-mer RNA hairpin, which has been specifically labeled with fluorine at the 2′-hydroxyl position of three ribose sugars. Experimentally measured ^{1}H-^{19}F dipolar couplings for the 2′-deoxy-2′-fluoro-sugars located in the helical region of the RNA hairpin were found to be in excellent agreement with values predicted using canonical A-form helical geometry, demonstrating that these couplings can provide accurate restraints for the refinement of RNA structures determined by NMR.

Abbreviations: RNA, ribonucleic acid; E.COSY, exclusive correlation spectroscopy; TOCSY, total correlation spectroscopy; MOCCA, *mo*dified phase-*c*ycled *Ca*rr-Purcell; SVD, singular value decomposition.

Introduction

Residual dipolar couplings can provide powerful through-space distance and angular restraints for the structure determination and refinement of macromolecules in solution (Tolman et al., 1995; Tjandra and Bax, 1997; Tjandra et al., 1997). In particular, residual dipolar couplings can significantly impact the precision to which global conformations are determined since these couplings afford unique long-range restraints that are absent in standard NOE and *J*-coupling measurements (Clore et al., 1998, 1999; Clore and Garrett, 1999; Olejniczak et al., 1999; Barrientos et al., 2000; Meiler et al., 2000; Skrynnikov et al., 2000; Tjandra et al., 2000). The application of residual dipolar couplings to nucleic acids, which have a significantly lower proton density when compared to proteins and normally lack NOEs relating nucleotides that are far apart in the primary sequence, can have an especially dramatic effect on the precision to which structures can be determined (Mollova et al., 2000; Tjandra et al., 2000; Vermeulen et al., 2000). Without NOEs or residual dipolar couplings to relate distal parts of nucleic acids, small errors in short-range restraints can propagate and result in large variations in the global conformation, even when the local geometry is rather precisely determined (Allain and Varani, 1997; Mollova et al., 2000).

Observation of residual dipolar couplings requires the partial alignment of macromolecules in solution. Such partial ordering can be achieved at ultrahigh magnetic fields for macromolecules with significant inherent magnetic anisotropy (Tolman et al., 1995; Tjandra et al., 1997) or through the use of anisotropic

*To whom correspondence should be addressed. E-mail: marino@carb.nist.gov

liquid crystalline media, such as magnetically oriented lipid bicelles, filamentous bacteriophage, and purple membranes (Tjandra and Bax, 1997; Clore et al., 1998; Hansen et al., 1998, 2000). Since liquid crystalline media can be tuned both to achieve an optimal range of measurable residual dipolar couplings and to alter the principal macromolecular alignment tensor (Hansen et al., 1998; Ottiger and Bax, 1998; Al-Hashimi et al., 2000), the use of these media now allows the routine measurement of residual dipolar couplings for almost any macromolecular system. Proteins and nucleic acids partially oriented by liquid crystalline media show sizeable residual dipolar couplings between one-bond separated ^{1}H-^{15}N and ^{1}H-^{13}C spin pairs, which are relatively easy to measure and apply in structure refinement (Tjandra and Bax, 1997; Clore et al., 1998; Hansen et al., 1998, 2000). For D_{XH} couplings, the difference in XH splitting observed for oriented versus isotropic samples can be used to measure the magnitude of the residual dipolar coupling, with the relative sign also determined so long as $D_{XH} < {}^{1}J_{XH}$. Interpretation of D_{XH} couplings is also rather straightforward since they are between nuclei separated by a known distance and therefore primarily a function of the orientation of the interatomic vector.

Long-range ^{1}H-^{1}H residual dipolar couplings are also observed in macromolecules partially oriented by liquid crystalline media and can be applied in structure refinement (Bolon and Prestegard, 1998; Ottiger et al., 1998; Cai et al., 1999; Carlomagno et al., 2000; Peti and Griesinger, 2000; Tian et al., 2000; Tjandra et al., 2000). These couplings can be measured either as an associated passive coupling (Cai et al., 1999; Peti and Griesinger, 2000) or employed as the active coupling via which unique magnetization transfer pathways can be achieved (Bolon and Prestegard 1998; Hansen et al., 1998; Tian et al., 1999, 2000). Although ^{1}H-^{1}H residual dipolar couplings offer the possibility of additional restraints for structural refinement, fitting these couplings is more challenging since they depend both on the distance between spins and the angle between the intermolecular vector and the principal alignment tensor. Moreover, severe overlap of proton resonances and multiple coupling partners, especially for RNA ribose protons, makes the practical measurement of ^{1}H-^{1}H couplings often difficult.

As an alternative to the measurement of ^{1}H-^{1}H residual dipolar couplings, we have explored methods for the measurement and application of residual ^{1}H-^{19}F dipolar couplings in the refinement of RNA solution structures. Sensitive X-filtered-E.COSY methods have been used to measure residual dipolar couplings between ^{1}H-^{19}F spin pairs in RNA, specifically fluorine labeled at the 2′-hydroxyl position of ribose (2′F-labeled) and aligned in solution using filamentous bacteriophage. The methods are demonstrated on a 21-mer RNA stem-loop, R1inv, derived from the *ColE1* plasmid encoded transcript RNA I (Eguchi et al., 1991). It is shown that experimentally measured ^{1}H-^{19}F dipolar couplings for 2′F-labeled ribose sugars located in the helical region of this RNA hairpin are in excellent agreement with values predicted based on canonical A-form helical geometry, demonstrating that these couplings can provide accurate restraints for the refinement of RNA solution structures determined by NMR.

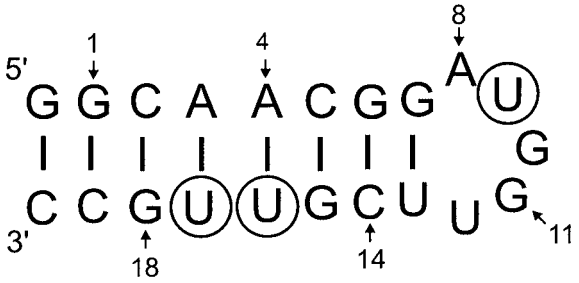

Scheme 1. Secondary structure of the 21-mer R1inv RNA hairpin. Hydrogen bonded base pairs are connected by solid lines. Selectively F2′-labeled positions [U9 (loop), U16 and U17 (stem)] are circled.

Materials and methods[1]

Sample preparation

The 21-mer R1inv hairpin (Scheme 1), specifically labeled with 2′F-U at positions 9, 16 and 17 in the sequence, was synthesized on an Applied Biosystems 390 synthesizer (Perkin-Elmer, Forest City, CA) using standard phosphoramidite chemistry (Beaucage and Caruthers, 1981). 2′F-U nucleoside phosphoramidite was purchased from Promega (Madison, WI). RNA oligonucleotides were deprotected using standard procedures, purified using preparative-scale denaturing polyacrylamide gel electrophoresis (PAGE) and recovered by electrophoretic elution. RNA samples were

[1]Certain commercial equipment, instruments, and materials are identified in this paper in order to specify the experimental procedure. Such identification does not imply recommendation or endorsement by the National Institute of Standards and Technology, nor does it imply that the material or equipment identified is necessarily the best available for the purpose.

desalted and dialyzed into a final buffer of 1 mM Cacodylate (pH = 6.5), 25 mM NaCl in 99.96% D_2O. The R1inv concentration was determined by measuring the absorbance at 260 nm using an extinction coefficient = 201.8 mM^{-1} cm^{-1}. The final concentration of the 2′F-labeled R1inv in the NMR samples was ∼ 1.0 mM. Filamentous bacteriophage, Pf1, was prepared using methods previously described (Hansen et al., 1998, 2000). Purified Pf1 stocks were concentrated and exchanged into a final buffer containing 10 mM d11-Tris (pH = 7.0) in 99.9% D_2O. To achieve alignment, Pf1 was added to the 2′F-labeled R1inv NMR sample to a final concentration of 12.5 mg/ml. Shigemi (Allison, PA) limited volume NMR tubes were used with a final total volume of ∼ 300 μL for each sample.

Measurement of ^{19}F, ^{1}H dipolar couplings

All NMR spectra were recorded on a Bruker AVANCE 500 MHz spectrometer (Bruker Instruments, Billerica, MA) equipped with a double-tuned ^{1}H,^{19}F probehead and processed using a Silicon Graphics O2 workstation. Two-dimensional ^{19}F filtered E.COSY spectra with various homonuclear transfer elements were recorded at 25 °C, using the pulse sequence schemes in Figure 1. The ^{19}F X-filtered-E.COSY-TOCSY spectra were collected using the DIPSI-2 isotropic mixing sequence (Shaka et al., 1988) with a spin lock period of 52 ms, with a 90° pulse of length 50 μs and sweep widths of 5000 Hz in ω_2 and 1700 Hz in ω_1, 1K by 128 complex data points in t_2 and t_1, respectively, and 192 scans per increment. ^{19}F X-filtered-E.COSY-NOESY spectra were collected with a mixing time of 300 ms and the same spectral parameters as the ^{19}F X-filtered-E.COSY-TOCSY. To achieve maximum Hartmann-Hahn-like transfer via dipolar couplings, ^{19}F X-filtered-E.COSY-TOCSY spectra were collected using a *mo*dified phase-*c*ycled *Ca*rr-Purcell-type, or so-called MOCCA, multiple pulse sequence (Kramer et al., 2001) as the homonuclear mixing block. The 180° pulses of the MOCCA-XY16 sequence were set to 40 μs surrounded by delays of 100 μs each with an overall mixing time of 268 ms.

Two-dimensional data were processed using NMRPipe (Delaglio et al., 1995) software. All two-dimensional spectra were apodized using 90° shifted sine bell functions over 512 and 256 complex points in the t_2 and t_1 dimensions, respectively and zero filled to 2K and 512 points in the two dimensions. Peak positions were determined through the use of the built-in peak picking routine of NMRDraw (Delaglio et al., 1995) and by looking at the relative displacement of contours at medium peak height, respectively.

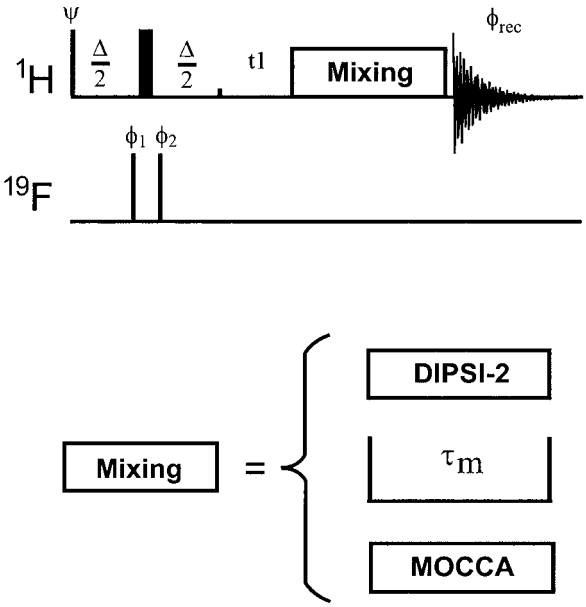

Figure 1. General pulse sequence scheme for the X-filtered-E.COSY experiment, consisting of a standard heteronuclear X-filter followed by a ^{1}H-^{1}H mixing step. Narrow and wide vertical lines indicate 90° and 180° flip angle pulses, respectively. All pulses are applied along x unless otherwise indicated. The experiment was employed with homonuclear DIPSI-2, NOESY and dipolar-TOCSY mixing steps. The residual HDO signal was suppressed by presaturation. The delay Δ was set to 19.6 ms. Phase cycle: ϕ_1 = x, −x; ϕ_2 = 2(x), 2(−x); ψ = x; Rec = (x, −x, −x, x). Quadrature detection is obtained in ω_1 by incrementing ψ according to States-TPPI. Additional parameters for the DIPSI-2, NOESY and dipolar-TOCSY mixing steps are given in Materials and methods. All spectra shown in Figure 3 were collected with 1024 (t_2^{max} = 204.5 ms) and 128 (t_1^{max} = 75.3 ms) complex points in ω_2 and ω_1, respectively, at 25 °C. The fluorine transmitter was centered at −201 ppm and the proton transmitter was centered on the residual HDO signal (4.75 ppm). 192 scans per t_1 increment were collected with spectral widths of 5000 and 1700 Hz in ω_2 and ω_1, respectively. Each experiment was run for ∼ 24 h using a ∼ 1.0 mM F2′-labeled R1inv sample either with or without Pf1.

Fitting ^{19}F,^{1}H dipolar couplings

Residual dipolar couplings assigned to the two fluorine nuclei substituted into ribose sugars at positions U16 and U17 within the helical stem region of the R1inv hairpin were fit using an idealized A-form model for the trinucleotide segment (U16, U17, G18) of the RNA (Figure 4). The couplings were fit to the trinucleotide segment, built using the program Insight II, by singular value decomposition (Losonczi et al., 1999)

and the program PALES (Zweckstetter and Bax, 2000) with the -bestFit option.

Results and discussion

X-filtered-E.COSY-type methods have been used to measure long-range dipolar coupling constants between ^{19}F-^{1}H spin pairs in RNA oligonucleotides aligned in solution using the filamentous bacteriophage, Pf1. Fluorine was chosen as an ideal heteronucleus for measuring long-range dipolar couplings in the context of the X-filtered-E.COSY experiments since ^{19}F is in 100% natural abundance and its gyromagnetic ratio is comparable to that of protons [$\gamma_F = 2.5181 \times 10^8$ (Ts)$^{-1}$ vs. $\gamma_H = 2.6752 \times 10^8$ (Ts)$^{-1}$]. Fluorine can therefore be used as a selective reporter for long-range ^{1}H-^{19}F dipolar interactions, while maintaining the sensitivity obtained in ^{1}H-^{1}H residual dipolar coupling measurements. In this study, selective fluorine substitution for the 2′-OH of ribose was chosen since it is well established that fluorine labeling at this position of the sugar favors a C3′-endo sugar pucker, which is normally found for A-form RNA geometry (Blandin et al., 1974; Reif et al., 1997). Thus, labeling at this position is expected to be nonperturbing for the canonical ribose sugar conformation found in most helical regions of RNA structure. In addition, the ^{19}F spectrum of the 2′F-labeled RNA was found to be well dispersed and could be utilized in multi-dimensional experiments to resolve ribose proton spectral overlap.

The E.COSY-type experiments (Griesinger et al., 1985, 1986) used here to measure long-range ^{19}F-^{1}H residual dipolar couplings (Figure 1) have been adopted from methods previously employed to measure long-range $^{n}J_{HX}$ couplings (Edison et al., 1991; Hines et al., 1993, 1994). The experiments are applied using a standard ^{19}F X-filter tuned to the $^{2}J_{H2',F2'}$ coupling of $\sim$ 51 Hz, which selects for fluorine coupled H2′ proton resonances. The X-filter is followed by evolution in t_1 of H2′ proton chemical shift and the $^{2}J_{H2',F}$ coupling. The H2′ proton magnetization is then correlated via a homonuclear mixing step to other protons, while leaving the spin state of the fluorine nucleus unperturbed. Lastly, the long-range correlated protons are acquired without ^{19}F decoupling. Figure 2A shows a schematic of a ribose sugar, highlighting the H2′,F *J*-coupled spin pair and indicating with arrows potential H2′,H spin pairs that are observed to be correlated via the homonuclear transfers. A schematic of the H,H correlated cross peak pattern expected from the ^{19}F X-filtered-E.COSY experiments is shown in Figure 2B. The cross peak scheme shows the multiplet displaced by the sum of the relatively large F-H2′ couplings ($^{2}J_{F2',H2'} + D_{F2',H2'}$) in the inverse t_1 dimension and the sum of smaller F-H dipolar couplings ($^{n}J_{F2',H} + D_{F2',H}$) in the t_2 dimension. Analysis of the displacement of the multiplets in t_2 yields the magnitude of the long-range dipolar coupling, while the tilt of the multiplet pattern yields the relative sign.

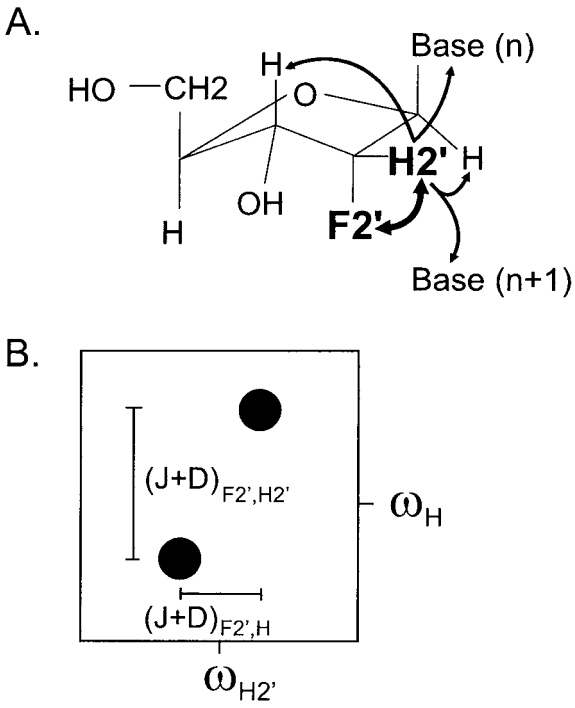

Figure 2. (A) Schematic of a 2′F-labeled ribose sugar with the F2′,H2′ spin pair connected by a bold arrow and potential long-range H2′,H transfer paths indicated by normal arrows. 2′-F labeling provides a 51 Hz geminal ^{19}F-^{1}H coupling to H2′ and allows the observation of residual dipolar ^{19}F-^{1}H couplings to both intra- and internucleotide ribose and aromatic base protons. (B) Schematic of the E.COSY pattern generated to determine the ^{19}F-^{1}H couplings, with the relatively large F2′-H2′ couplings evolved in the indirect dimension to resolve the smaller long-range F2′-H couplings in the directly detected dimension.

Homonuclear ^{1}H NOESY (Macura et al., 1982), DIPSI-2 (Shaka et al., 1988) and dipolar-TOCSY (Kramer et al., 2001) mixing elements were used in the experiments in this study. In principle, other homonuclear magnetization transfer steps could also have been implemented, including for example COSY or ROESY, to achieve the ^{1}H-^{1}H correlations. In practice, however, it was found that NOESY and dipolar-

TOCSY mixing elements provided the most effective transfer of magnetization. For the dipolar-TOCSY version of the X-filtered-E.COSY experiment, a new class of CPMG-related TOCSY sequences, or so-called MOCCA sequences (Kramer et al., 2001), was used. Since the dipolar coupling Hamiltonian is anisotropic [for a two-spin system, $H_{Dipolar} = 2\pi\ D(2I_zS_z - I_xS_x - I_yS_y)$, where D is the dipolar coupling between spins I and S], conventional TOCSY sequences, like DIPSI-2, which are optimized for isotropic mixing in *J*-coupled spin systems, are not well suited for the correlation of dipolar coupled spins. Under the dipolar coupling Hamiltonian, most commonly used isotropic TOCSY sequences, such as DIPSI-2, result in a reduction of the effective transfer efficiency due to a scaling of the effective dipolar coupling by a factor of $-1/2$ [for a two-spin system, the effective dipolar coupling Hamiltonian for DIPSI-2 applied along the x-axis is of the form $H_{DipolarCW} = 2\pi D(I_xS_x - (I_zS_z + I_yS_y))$] (Kramer et al., 1999, 2001; Luy and Glaser, 2000, 2001). In addition, isotropic TOCSY sequences result in an offset behavior that is completely different from that observed in *J*-coupled systems (Kramer et al., 1999).

The MOCCA-XY16 sequence used here is based on a multiple pulse-delay design. For this sequence the scaling of the effective dipolar coupling Hamiltonian is approximately 0.75 and the offset dependence shows the desired square-like shape (Kramer et al., 2001). Additionally, care has to be taken in choosing the best orientation for the magnetization with respect to the principal axis system of the effective dipolar coupling tensor, since the dipolar coupling Hamiltonian is generally of cylindrical symmetry. It was found that the efficiency of magnetization transfer, which can be derived from coherence transfer functions, differs strongly for transfer along the principal axis (z for MOCCA sequences) versus in the plane (x or y for MOCCA sequences) and generally depends on the coupling topology of the spin system (Luy and Glaser, 2000, 2001). From inspection of the analytical transfer functions of spin systems containing up to three spins it appears that for most spin systems the transfer along the principal axis is preferable. Therefore, the MOCCA-XY16 sequence with the magnetization locked along the z-axis was used for the mixing step. Since magnetization is locked along the principal axis, implementation of this version of the MOCCA sequence had the added benefit of showing very favorable relaxation behavior, which approached longitudinal relaxation rates.

To demonstrate measurement and application of ^{19}F-^{1}H residual dipolar couplings in the structure determination and refinement of RNA, a 21-mer RNA hairpin (Scheme 1) was used that was specifically labeled at the 2′ hydroxyl position of three ribose sugars (U9, U16 and U17). To ensure that fluorine labeling did not significantly affect the functional properties of the R1inv stem-loop, the binding properties of 2′F-R1inv to its complement R2inv were determined using a fluorescence detected binding assay. Using this assay, 2′F-R1inv was shown to bind R2inv and form a loop–loop 'kissing' complex (Eguchi et al., 1991; Marino et al., 1995; Lee and Crothers, 1998) with a K_D that was comparable to unlabeled RNA stem-loop constructs (data not shown), thus providing evidence that the ^{19}F-labeling was in general non-perturbing. Representative cross peaks obtained from ^{19}F X-filtered-E.COSY experiments applied to the 2′F-labeled R1inv stem-loop using NOESY and dipolar-TOCSY mixing elements are shown in Figure 3. In general, cross peaks were well resolved in these spectra due to use of a limited number (3) of selective fluorine labels and the added dispersion in the proton spectra afforded by 2′F-labeled ribose sugars. Since it is optimized to correlate spins via dipolar couplings, the MOCCA sequence was observed to give additional correlations not found in the X-filtered-E.COSY experiments that employed either the NOESY or DIPSI-2 mixing elements (Figure 3). Taken together, the three mixing sequences used for the homonuclear transfer step allowed the measurement of a number of long-range residual dipolar ^{19}F-^{1}H-couplings for the R1inv hairpin, which could be used as restraints in structure refinement. The isotropic ^{1}H-^{19}F *J*-couplings observed by applying the NOESY version of the experiment to an R1inv hairpin, as well as the sum of the ^{1}H-^{19}F dipolar and *J*-couplings observed by applying the dipolar-TOCSY and NOESY versions of the experiment to an oriented R1inv hairpin are given in Table 1. The residual dipolar couplings determined from the difference between the F-H splitting observed for the isotropic versus oriented samples are also given in bold in Table 1. These calculated values represent an average of the different experimental measurements.

To test the accuracy of the measured ^{19}F-^{1}H residual dipolar couplings, the couplings associated with residues U16 and U17, located in the helical stem region of the R1inv hairpin were fit using a model trinucleotide built with canonical A-form geometry (Figure 4A). The six couplings measured for these two

Table 1. Measured scalar and dipolar HF couplings

Cross peak	F-H coupled spins	D-TOCSY w/ Pf1 $\Sigma D_{HF} + J_{HF}$ (Hz)	NOESY w/ Pf1 $\Sigma D_{HF} + J_{HF}$ (Hz)	NOESY w/o Pf1 J_{HF} (Hz)	D_{HF} (Hz)
H2′[U9] - H1′[U9]	2′F[U9]-H1′[U9]	13.0	13.0	17.4	**−4.4**
H2′[U9] - H2′[U9]	2′F[U9]-H2′[U9]	54.0	54.0	51.5	**2.5**
H2′[U9] - H3′[U9]	2′F[U9]-H3′[U9]	17.0	16.8	20.5	**−3.6**
H2′[U9] - 7.52 ppm	2′F[U9]-H[7.52 ppm]	−0.6	–	0	**−0.6**
H2′[U9] - 8.17 ppm	2′F[U9]-H[8.17 ppm]	1.2	–	–	**1.2**
H2′[U16] - H1′[U16]	2′F[U16]-H1′[U16]	8.5	8.6	14.0	**−5.4**
H2′[U16] - H2′[U16]	2′F[U16]-H2′[U16]	53.7	53.5	50.6	**3.0**
H2′[U16] - 5.74 ppm	2′F[U16]-H[5.74 ppm]	∼1.0	∼1.0	0	**1.0**
H2′[U16] - H6[U17]	2′F[U16]-H6[U17]	0.5	0.7	0	**0.6**
H2′[U17] - H1′[U17]	2′F[U17]-H1′[U17]	7.9	7.8	14.1	**−6.2**
H2′[U17] - H2′[U17]	2′F[U17]-H2′[U17]	54.0	54.5	50.5	**3.8**
H2′[U17] - 5.86 ppm	2′F[U17]-H[5.86 ppm]	−0.8	−1.0	0	**−0.9**
H2′[U17] - 5.97 ppm	2′F[U17]-H[5.97 ppm]	−1.2	–	–	**−1.2**
H2′[U17] - H8[G18]	2′F[U17]-H8[G18]	1.1	1.0	0	**1.1**

The estimated error in the coupling constant determination varies from ±0.2 Hz for strong cross peaks to ±0.6 Hz for weaker peaks and peaks with complex multiplet patterns. For unassigned cross peaks, proton chemical shifts are given in ppm.

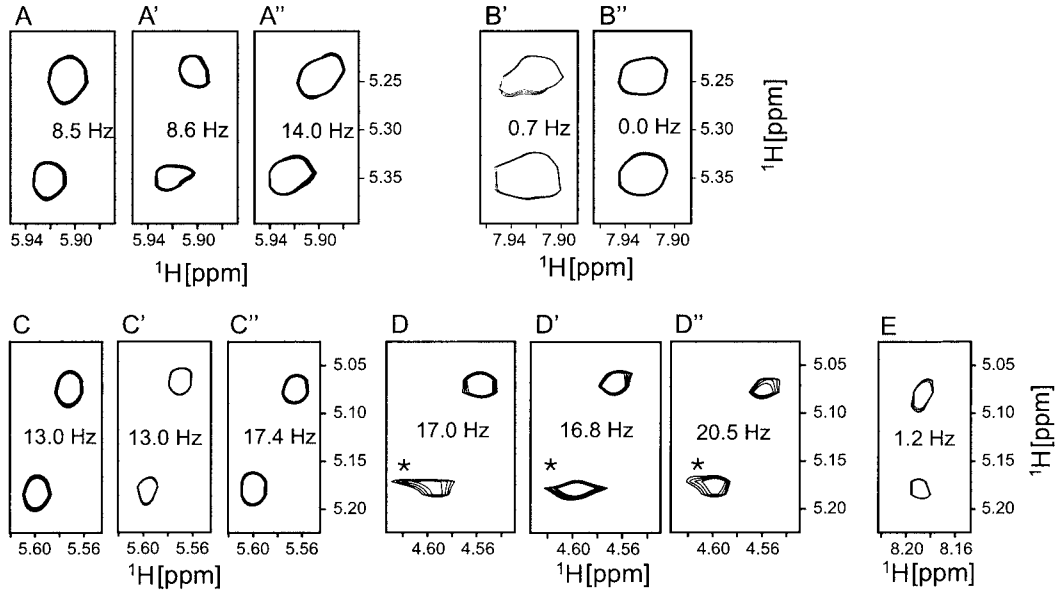

Figure 3. Representative cross peaks (A–E) chosen from ^{19}F X-filter-E.COSY experiments using NOESY and dipolar-TOCSY mixing elements. A plain letter (e.g. A) is used to indicate cross peaks generated using the dipolar-TOCSY version of the experiment on an aligned sample, a prime (e.g. A′) is used to indicate cross peaks generated using the NOESY version of the experiment on an aligned sample and a double-prime (e.g. A″) is used to indicate cross peaks generated using the NOESY version of the experiment on an unaligned sample. The cross peaks shown are: H2′[U16]-H1′[U16] (A, A′, A″), H2′[U16]-H6[U17] (B′,B″), H2′[U9]-H1′[U9] (C, C′, C″), H2′[U9]-H3′[U9] (D, D′,D″), and H2′[U9]-8.17 ppm (E). A few cross peaks are weakened by complex multiplet patterns which result from a number of moderately strong ^{1}H-^{1}H dipolar couplings (e.g. B′), but are still measurable. The use of MOCCA mixing provided transfer to some protons that were beyond detection in the corresponding NOESY experiments (e.g. E), but sometimes yielded a weaker cross peak (e.g. H2′[U16]-H6[U17] correlation). The asterisks indicate artifacts resulting from residual water. A list of experimental dipolar couplings is given in Table 1.

residues were fit using a singular value decomposition (SVD) algorithm (Losonczi et al., 1999) leading to a clearly identified alignment tensor (data not shown). With the model trinucleotide sequence and the experimental couplings as input for the program PALES (Zweckstetter and Bax, 2000), the dipolar couplings of U16 and U17 were fit such that an excellent agreement (Figure 4B) could be achieved between experimental and calculated couplings (rmsd = 0.04 Hz). Since a small number of couplings were used in the fitting procedure, the sensitivity of the fit to variation in measured dipolar couplings was tested by systematically varying the measured couplings in 1 Hz increments (−2 Hz, −1 Hz, 1 Hz, 2 Hz) and repeating the PALES fitting routine. Using this procedure it was found that the changes of ±1 and ±2 Hz in a single measured coupling significantly increased the best possible rmsd to values ranging between 0.2–1.2 Hz and 0.4–2.4 Hz, respectively. In these tests, it was found that changes in dipolar couplings which are close to zero in magnitude, where the couplings are especially sensitive to local RNA conformation, could give rise to rmsd values that are slightly larger than the actual change in the coupling itself. The fitting procedure was also verified by refitting the data after single pairwise exchanges of the coupling assignments. In all cases tested, the rmsd was again determined to increase significantly (ranging from 0.4 to 5.4 Hz) from the 0.04 rmsd found for the correct assignments and couplings. A full description of the tests of the PALES fitting routine is available as supplemental information. The rather good fit between experimental data and values simulated based on A-form geometry was expected since the helical region of this hairpin is known to be in an A-form helical conformation and the C3′-endo conformation adopted by ribose sugars in A-form geometry is known to be stabilized by ^{19}F substitution at the 2′-OH position.

Although ^{19}F substitution in canonical A-form regions of RNA structure does not provide novel long-range information within a particular RNA helix, the measurement of ^{19}F-^{1}H dipolar couplings can be used as a tool for quick measurement of inter-helical orientation in large RNA molecules and complexes. As demonstrated here, a few selective ^{19}F labels can be rapidly assigned and used to generate a sufficient number of dipolar couplings to determine helical orientation in large RNA structures. Other advantages of selective ^{19}F labeling in studying larger RNA molecules are that ^{19}F correlated/edited ^{1}H spectra are often better resolved than ^{13}C and ^{15}N correlated spectra and relaxation of ^{1}H due to ^{13}C incorporation is more significant relative to ^{19}F labeling. In addition, ^{1}H-^{19}F dipolar couplings provide unique projection angles in helical regions of RNA structure that are non-redundant with those angles derived from ^{13}C-^{1}H and ^{15}N-^{1}H dipolar couplings.

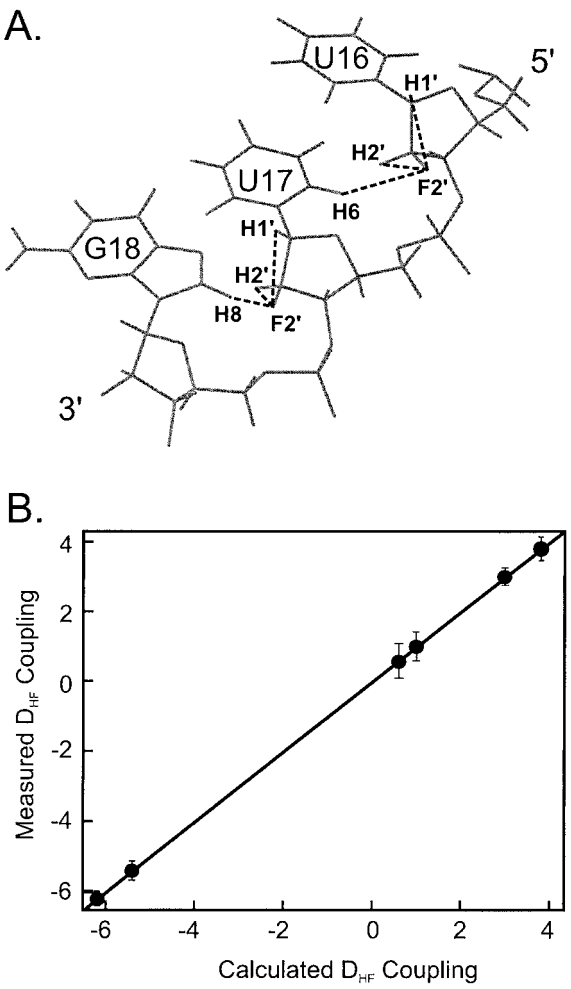

Figure 4. (A) Structure of a UUG trinucleotide built with canonical A-form geometry using Insight II (MSI Inc.). The assigned residual dipolar couplings shown as dashed lines were fitted using this structural element by singular value decomposition (Losonczi et al., 1999) and the program PALES (Zweckstetter and Bax, 2000). (B) Plot of the correlation between the experimentally determined and calculated ^{19}F-^{1}H dipolar couplings. The straight line is a least-squares fit of the data.

Since a good structural model for the loop region of the R1inv hairpin is not currently available, the ^{19}F-^{1}H residual dipolar couplings associated with 2′F-labeled U9 ribose sugar could not be readily fit. Moreover, fluorine substitution was found to perturb the previously determined equilibrium population distribution of C2′-

versus C3′-endo sugar pucker for the U9 ribose, resulting in a shift towards a higher population of C3′-endo pucker. Thus, although ^{19}F-^{1}H residual dipolar couplings associated with residue U9 were measured and could potentially provide structural information on the loop conformation, the use of these couplings was not pursued.

Conclusions

We have synthesized selectively 2′F-labeled RNA and demonstrated sensitive X-filtered-E.COSY methods for the sign-sensitive measurement of long-range ^{19}F-^{1}H residual dipolar couplings. For 2′F-labeled ribose sugars in the helical region of the R1inv structure, experimentally determined dipolar couplings could be fit using SVD within the program PALES and were found to be in excellent agreement with the calculated couplings based on ideal A-form geometry. In contrast, 2′F-labeling of a ribose sugar in the loop region of the R1inv structure resulted in a perturbation of the sugar conformational equilibrium, demonstrating the limitation of 2′F-labeling in non-canonical regions of RNA structure. Since labeling in the helical regions of the R1inv structure was found to be structurally non-perturbing and could be fit accurately, we anticipate that selective 2′F-labeling of ribose sugars in different helical regions of an RNA structure could be used to determine the relative orientations of helices in the global fold. Applied in this way, the measurement of ^{1}H-^{19}F dipolar couplings could provide a general method for determining accurate restraints for the refinement of the global structure of RNA in solution.

Acknowledgements

This work was supported by NIH (GM 59107-01) to J.P.M. B.L. acknowledges a Feodor Lynen fellowship from the AvH-Stiftung. We thank Dr. F. Song (CARB) for synthesis of ^{19}F labeled RNA, Dr. J. Barchi Jr. (NCI/NIH) for use of his ^{1}H/^{19}F NMR probehead and insightful discussions, Prof. A. Pardi (University of Colorado) for providing Pf1 starter cultures, Dr. A. Fowler (Yale University) for his help with SVD, Dr. M. Zweckstetter (NIH) for providing an extension of his program PALES, F. Kramer and S.J. Glaser (TU-München) for making the MOCCA sequences available prior to publication and for interesting discussions and M. Rist (CARB) for fluorescence measurements.

References

Al-Hashimi, H.M., Valafar, H., Terrell, M., Zartler, E.R., Eidsness, M.K. and Prestegard, J.H. (2000) *J. Magn. Reson.*, **143**, 402–406.
Allain, F.H. and Varani, G. (1997) *J. Mol. Biol.*, **267**, 338–351.
Barrientos, L.G., Dolan, C. and Gronenborn, A.M. (2000) *J. Biomol. NMR*, **16**, 329–337.
Beaucage, S.L. and Caruthers, M.H. (1981) *Tetrahedron Lett.*, **22**, 1859.
Blandin, M., Son, T., Catlin, J. and Guschlbauer, W. (1974) *Biochim. Biophys. Acta*, **361**, 249–256.
Bolon, P.J. and Prestegard, J.H. (1998) *J. Am. Chem. Soc.*, **120**, 9366–9367.
Cai, M.L., Wang, H., Olejniczak, E.T., Meadows, R.P., Gunasekera, A.H., Xu, N. and Fesik, S.W. (1999) *J. Magn. Reson.*, **139**, 451–453.
Carlomagno, T., Peti, W. and Griesinger, C. (2000) *J. Biomol. NMR*, **17**, 99–109.
Clore, G.M. and Garrett, D.S. (1999) *J. Am. Chem. Soc.*, **121**, 9008–9012.
Clore, G.M., Gronenborn, A.M. and Tjandra, N. (1998) *J. Magn. Reson.*, **131**, 159–162.
Clore, G.M., Starich, M.R., Bewley, C.A., Cai, M.L. and Kuszewski, J. (1999) *J. Am. Chem. Soc.*, **121**, 6513–6514.
Clore, G.M., Starich, M.R. and Gronenborn, A.M. (1998) *J. Am. Chem. Soc.*, **120**, 10571–10572.
Delaglio, F., Grzesiek, S., Vuister, G.W., Zhu, G., Pfeifer, J. and Bax, A. (1995) *J. Biomol. NMR*, **6**, 277–293.
Edison, A.S., Westler, W.M. and Markley, J.L. (1991) *J. Magn. Reson.*, **92**, 434–438.
Eguchi, Y., Itoh, T. and Tomizawa, J. (1991) *Annu. Rev. Biochem.*, **60**, 631–652.
Griesinger, C., Sørensen, O.W. and Ernst, R.R. (1986) *J. Chem. Phys.*, **85**, 6837–6852.
Griesinger, C., Sørensen, O.W. and Ernst, R.R. (1985) *J. Am. Chem. Soc.*, **107**, 6394–6396.
Hansen, M.R., Hanson, P. and Pardi, A. (2000) *Methods Enzymol.*, **317**, 220–240.
Hansen, M.R., Mueller, L. and Pardi, A. (1998) *Nat. Struct. Biol.*, **5**, 1065–1074.
Hansen, M.R., Rance, M. and Pardi, A. (1998) *J. Am. Chem. Soc.*, **120**, 11210–11211.
Hines, J.V., Landry, S.M., Varani, G. and Tinoco Jr, I. (1994) *J. Am. Chem. Soc.*, **116**, 5823–5831.
Hines, J.V., Varani, G., Landry, S.M. and Tinoco Jr, I. (1993) *J. Am. Chem. Soc.*, **115**, 11002–11003.
Kramer, F., Luy, B. and Glaser, S.J. (1999) *Appl. Magn. Reson.*, **17**, 173–187.
Kramer, F., Peti, W., Griesinger, C. and Glaser, S.J. (2001) *J. Magn. Reson.*, **149**, 58–66.
Lee, A. and Crothers, D. (1998) *Structure*, **6**, 993–1005.
Losonczi, J.A., Andrec, M., Fischer, M.W.F. and Prestegard, J.H. (1999) *J. Magn. Reson.*, **138**, 334–342.
Luy, B. and Glaser, S.J. (2000) *J. Magn. Reson.*, **142**, 280–287.
Luy, B. and Glaser, S.J. (2001) *J. Magn. Reson.*, **148**, 169–181.
Macura, S., Wüthrich, K. and Ernst, R.R. (1982) *J. Magn. Reson.*, **46**, 269–282.
Marino, J.P., Gregorian, R.S., Csankovszki, G. and Crothers, D.M. (1995) *Science*, **268**, 1448–1454.

Meiler, J., Blomberg, N., Nilges, M. and Griesinger, C. (2000) *J. Biomol. NMR*, **16**, 245–252.

Mollova, E.T., Hansen, M.R. and Pardi, A. (2000) *J. Am. Chem. Soc.*, **122**, 11561–11562.

Olejniczak, E.T., Meadows, R.P., Wang, H., Cai, M.L., Nettesheim, D.G. and Fesik, S.W. (1999) *J. Am. Chem. Soc.*, **121**, 9249–9250.

Ottiger, M. and Bax, A. (1998) *J. Biomol. NMR*, **12**, 361–372.

Ottiger, M., Delaglio, F., Marquardt, J.L., Tjandra, N. and Bax, A. (1998) *J. Magn. Reson.*, **134**, 365–369.

Peti, W. and Griesinger, C. (2000) *J. Am. Chem. Soc.*, **122**, 3975–3976.

Reif, B., Wittmann, V., Schwalbe, H., Griesinger, C., Worner, K., Jahn-Hofmann, K. and Engels, J.W. (1997) *Helv. Chim. Acta*, **80**, 1952–1971.

Shaka, A.J., Lee, C.J. and Pines, A. (1988) *J. Magn. Reson.*, **77**, 274–293.

Skrynnikov, N.R., Goto, N.K., Yang, D.W., Choy, W.Y., Tolman, J.R., Mueller, G.A. and Kay, L.E. (2000) *J. Mol. Biol.*, **295**, 1265–1273.

Tian, F., Bolon, P.J. and Prestegard, J.H. (1999) *J. Am. Chem. Soc.*, **121**, 7712–7713.

Tian, F., Fowler, C.A., Zartler, E.R., Jenney, F.A., Adams, M.W. and Prestegard, J.H. (2000) *J. Biomol. NMR*, **18**, 23–31.

Tjandra, N. and Bax, A. (1997) *Science*, **278**, 1111–1114.

Tjandra, N., Marquardt, J. and Clore, G.M. (2000) *J. Magn. Reson.*, **142**, 393–396.

Tjandra, N., Omichinski, J., Gronenborn, A., Clore, G. and Bax, A. (1997) *Nat. Struct. Biol.*, **4**, 732–738.

Tjandra, N., Tate, S., Ono, A., Kainosho, M. and Bax, A. (2000) *J. Am. Chem. Soc.*, **122**, 6190–6200.

Tolman, J., Flanagan, J., Kennedy, M. and Prestegard, J. (1995) *Proc. Natl. Acad. Sci. USA*, **92**, 9279–9283.

Vermeulen, A., Zhou, A. and Pardi, A. (2000) *J. Am. Chem. Soc.*, **122**, 9638–9647.

Zweckstetter, M. and Bax, A. (2000) *J. Am. Chem. Soc.*, **122**, 3791–3792.